Introduction to Dynamic Models for Robot Force Control

Steven D. Eppinger and Warren P. Seering

ABSTRACT: Endpoint compliance strategies for precise robot control utilize feedback from a force sensor located near the tool/workpiece interface. The closed-loop performance of such endpoint force control systems has been observed in the laboratory to be limited and unsatisfactory for industrial applications. This article discusses the particular dynamic properties of robot systems that can lead to instability and limit performance. A series of lumped-parameter models is developed in an effort to predict the closed-loop dynamics of a force-controlled single-axis arm. The models include some effects of robot structural dynamics, sensor compliance, and workpiece dynamics. The qualitative analysis shows that the robot dynamics contribute to force-controlled instability. Recommendations are made for models to be used in control system design.

Introduction

Certain robot tasks demand precise interaction between the manipulator and its environment. Among these are many of the operations required in the mechanical assembly process. Strategies for the execution of such tasks involve controlling the relationship between endpoint forces and displacements under the environmentally imposed constraints. This endpoint *compliance* can be implemented in many different schemes, and Whitney [2] provides an overview of these. Strictly speaking, *compliance* is the inverse of stiffness; however, the term *compliant control* is often used to refer to any force control algorithm, since they use sensed force to alter controller commands.

Endpoint compliant control strategies depend on force signals measured by a wrist sensor. The sensor output is fed back to the controller to alter the system's performance. Many such closed-loop systems have been built using various force control algorithms, and many stability problems have been observed. A theoretical treatment of environmentally imposed constraints is provided by Mason [3], who also suggests a control methodology to augment these "natural" constraints with an appropriate set of "artificial" constraints. Raibert and Craig [4] developed a hybrid control architecture capable of implementing Mason's theory. Salisbury's stiffness control [5] regulates the end effector's stiffness in Cartesian coordinates using an appropriately formed joint stiffness matrix. Other compliant control strategies include Whitney's damping control [6] and Hogan's impedance control [7]. The simplest force control strategy is explicit force control [8], which makes no use of position feedback information in the controller, and the servo loop is based on force errors.

Active force control systems implemented to test these strategies have demonstrated dynamic stability problems. In practice, force-controlled robots do not have bandwidth sufficient for most industrial applications. Historically, some instabilities have been caused by digital sampling, and Whitney [2] discusses these conditions. Researchers have also observed the effects of unmodeled (uncompensated) nonlinearities, such as friction or backlash [9]. Raibert and Craig [4] implemented their hybrid controller and found oscillations present in the controlled system. Instabilities have been observed in the operation of both of the force-controlled robots currently in use at the MIT Artificial Intelligence (AI) Laboratory. These robots include a PUMA arm and the new MIT Precision Assembly Robot. Both arms display performance differences when the workpiece (environment) characteristics are changed.

Roberts et al. [10] investigated the effect of wrist sensor stiffness on the closed-loop system dynamics; they also included drive stiffness (transmission compliance) in their dynamic model. Transmission compliance causes the joint actuators and wrist sensors to be *noncolocated*, a condition discussed in detail by Gevarter [11]. Noncolocation is the stability problem that occurs when a control loop is closed using a sensor and an actuator placed at different points on a dynamic structure. Cannon [12] has investigated the similar problem of the position control of a flexible arm with endpoint sensing. He has shown that a high-order compensator is able to stabilize the system, but with limited bandwidth and high sensitivity to parameter changes. Sweet and Good [13] obtained realistic robot/transmission system dynamics from experimental tests and then included the influence of these effects in the controller design.

Researchers have named many suspected causes of the instabilities observed in force-controlled robot systems. Among these are: low digital sampling rate, filtering, workpiece dynamics, environment stiffness, actuator bandwidth, sensor dynamics, arm flexibility, impact forces upon tool/workpiece contact, and drive train backlash or friction. This article addresses the effects of arm, sensor, and workpiece dynamics.

Using conventional modeling and analysis techniques, it is demonstrated that when the arm flexibility gives rise to a vibratory mode within the desired closed-loop bandwidth, instability can occur. In particular, a simple, one-axis force control algorithm exhibits stable behavior when the higher-order dynamics of the arm can be neglected, and it can be unstable if those effects are significant. This is believed to be the cause of the instabilities observed in the robots at the MIT AI Laboratory.

Unstable behavior often takes the form of a limit cycle where the robot is making and breaking contact with the workpiece. In this article, the terms *workpiece* and *environment* are used interchangeably. The workpiece is the component of the environment contacted by the end effector of the force-controlled robot system. The discontinuous nature of this response makes the system difficult to model using linear elements. However, for the purposes of controller design, we will neglect the discontinuity and study linear system models. Nonlinear simulations (not

Steven D. Eppinger and Warren P. Seering are with the Artificial Intelligence Laboratory of the Massachusetts Institute of Technology, 545 Technology Square, Cambridge, MA 02139. This article describes research done at the Artificial Intelligence Laboratory of the Massachusetts Institute of Technology. Support for the laboratory's artificial intelligence research is provided in part by the System Development Foundation and in part by the Advanced Research Projects Agency of the Department of Defense under Office of Naval Research Contract N00014-85-K-0124. Support for this research project is also provided in part by the TRW Foundation. The original version of this paper was presented at the IEEE International Conference on Robotics and Automation in San Francisco, California, April 7-10, 1986 [1].

0272-1708/87/0400-0048 $01.00 © 1987 IEEE

presented in this paper) suggest that if the linearized system has sufficient damping, then neglecting the discontinuity is justified. However, if the linearized system has unstable or highly oscillatory closed-loop poles, then the discontinuity should be included in the model so that limit cycles can be predicted in simulation. For control system design, this analysis assumes that the robot endpoint remains in contact with the workpiece. Note that choosing control gains that give desirable response assures that we will not have unstable or highly oscillatory systems, and so the arm is likely to remain in contact.

Rigid-Body Robot Model

To begin with a simple case, let us consider the robot to be a rigid body, with no vibrational modes. Let us also consider the workpiece to be rigid, having no dynamics. The sensor connects the two with some compliance, as shown in Fig. 1. Throughout the model development, the term *robot* refers to the arm itself. The term *robot system* refers to the total system, comprised of the robot, sensor, workpiece, and controller.

We model the robot as a mass with a damper to ground. The mass m_r represents the effective moving mass of the arm. The viscous damper b_r is chosen to give the appropriate rigid-body mode to the unattached robot. While structural damping is very low, b_r includes the linearized effects of all of the other damping in the robot. The sensor has stiffness k_s and damping b_s. The workpiece is shown as a "ground state." The robot actuator is represented by the input force F, and the state variable x_r measures the position of the robot mass.

The open-loop dynamics of this simple system are described by the following transfer function:

$$X_r(s)/F(s) = 1/[m_r s^2 + (b_r + b_s)s + k_s]$$

Since this robot system is to be controlled to maintain a desired contact force, we must recognize that the closed-loop system output variable is the force across the sensor, the contact force F_c.

$$F_c = k_s x_r$$

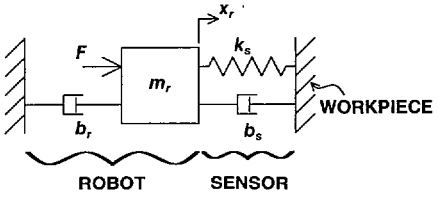

Fig. 1. Rigid-body robot model with compliant sensor and rigid workpiece.

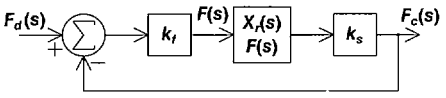

Fig. 2. Block diagram for the controller of Fig. 1.

We will now implement the simple proportional force control law:

$$F = k_f(F_d - F_c), \quad k_f \geq 0$$

which states that the actuator force should be some nonnegative force feedback gain k_f times the difference between some desired contact force F_d and the actual contact force. This control law is embodied in the block diagram of Fig. 2. The closed-loop transfer function then becomes

$$F_c(s)/F_d(s) = k_f k_s/[m_r s^2 + (b_r + b_s)s + k_s(1 + k_f)]$$

The control loop modifies the characteristic equation only in the stiffness term. The force control for this simple case works like a position servo system. This could have been predicted from the model in Fig. 1 by noting that the contact force depends solely on robot position x_r.

For completeness, let us look at the root locus plot for this system. Figure 3 shows the positions in the s plane of the roots of the closed-loop characteristic equation as the force feedback gain k_f varies. For this qualitative analysis, the model parameter values have been chosen only to plot root locus *shapes* representative of robot systems. They do not correspond to data taken from any specific robot. For this reason, the plots do not contain numerical markings on the axes. For $k_f = 0$, the roots are at the open-loop poles. The loci show that as the gain is increased, the natural frequency increases, and the damping ratio decreases, but the system remains stable. In fact, k_f can be chosen to give the controlled system desirable response characteristics.

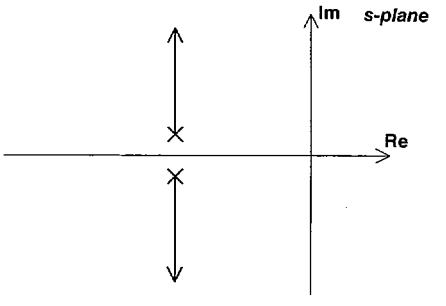

Fig. 3. Root locus plot shape for the controller of Fig. 1.

Include Workpiece Dynamics

The simple robot system of Fig. 1 has been shown to be unconditionally stable (for $k_f \geq 0$). Force-controlled systems, however, have been observed to exhibit variations in dynamic behavior, depending upon the characteristics of the workpiece with which the robot is in contact. It is with this phenomenon in mind that the robot system model is augmented to include workpiece dynamics, as shown in Fig. 4.

This two-mass model includes the same robot and sensor models used previously, with the workpiece now represented by a mass m_w. The workpiece is supported by a spring and damper to ground with parameters k_w and b_w, respectively. The new state variable x_w measures the position of the workpiece mass.

The open-loop transfer functions of this two-degree-of-freedom system are:

$$X_r(s)/F(s) = N_w(s)/D_4(s)$$

$$X_w(s)/F(s) = [b_s s + k_s]/D_4(s)$$

where

$$N_w(s) = [m_w s^2 + (b_s + b_w)s + (k_s + k_w)]$$

$$D_4(s) = [m_r s^2 + (b_r + b_s)s + k_s] \cdot N_w(s) - [b_s s + k_s]^2$$

The output variable is again the contact force F_c, which is the force across the sensor, given by

$$F_c = k_s(x_r - x_w)$$

If we now implement the same simple force controller, the control law remains unchanged.

$$F = k_f(F_d - F_c), \quad k_f \geq 0$$

The block diagram for this control system is shown in Fig. 5. Note that the feedforward path includes the difference between the two open-loop transfer functions.

The root locus for this system is plotted in Fig. 6 as the force feedback gain k_f is varied. There are four open-loop poles and two open-loop zeros. The plot then still has two asymptotes, at ± 90 deg. The shape of this root locus plot tells us that even for high

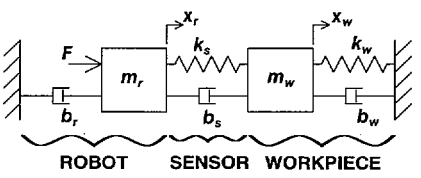

Fig. 4. Rigid-body robot model including workpiece dynamics.

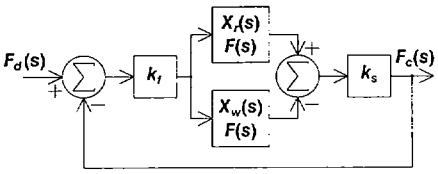

Fig. 5. Block diagram for the controller of Fig. 4.

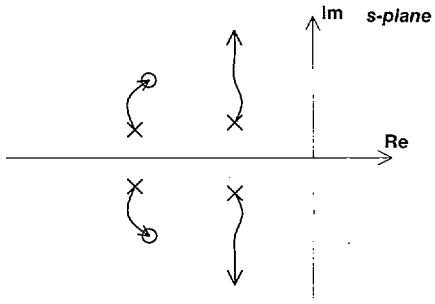

Fig. 6. Root locus plot shape for the controller of Fig. 4.

values of gain, the system has stable roots. Therefore, while the characteristics of the workpiece affect the dynamics of the robot system, they do not cause unstable behavior.

Include Robot Dynamics

Since the addition of the workpiece dynamics to the simple robot system model did not result in the observed instability, we will augment our system with a more complex robot model. If we wish to include both the rigid-body and first vibratory modes of the arm, then the robot alone must be represented by two masses.

Figure 7 shows the new system model. The total robot mass is now split between m_1 and m_2. The spring and damper with values k_2 and b_2 set the frequency and damping of the robot's first mode, while the damper to ground, b_1, primarily governs the rigid-body mode. The stiffness between the robot masses could be the drive train or transmission stiffness, or it could be the structural stiffness of a link. The masses m_1 and m_2 would then be chosen accordingly. The sensor and workpiece are modeled in the same manner as in Fig. 4. The three state variables

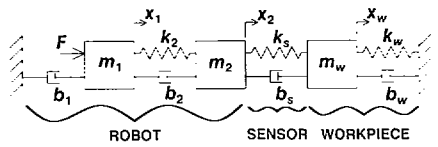

Fig. 7. Robot system model including robot first-mode and workpiece dynamics.

x_1, x_2, and x_w measure the positions of the masses m_1, m_2, and m_w.

This three-mass model has the following open-loop transfer functions:

$$X_1(s)/F(s) = N_4(s)/D_6(s)$$

$$X_2(s)/F(s) = N_3(s)/D_6(s)$$

$$X_w(s)/F(s) = N_2(s)/D_6(s)$$

where

$$N_4(s) = [m_2s^2 + (b_2 + b_s)s + (k_2 + k_s)] \cdot N_w(s) - [b_ss + k_s]^2$$

$$N_3(s) = N_w(s)[b_2s + k_2]$$

$$N_2(s) = [b_2s + k_2][b_ss + k_s]$$

$$D_6(s) = [m_1s^2 + (b_1 + b_2)s + k_2] \cdot [m_2s^2 + (b_2 + b_s)s + (k_2 + k_s)] \cdot N_w(s) - N_w(s)[b_2s + k_2]^2 - [m_1s^2 + (b_1 + b_2)s + k_2] \cdot [b_ss + k_s]^2$$

$$N_w(s) = [m_ws^2 + (b_s + b_w)s + (k_s + k_w)]$$

The contact force is again the force across k_s

$$F_c = k_s(x_2 - x_w)$$

and the simple force control law is

$$F = k_f(F_d - F_c), \quad k_f \geq 0$$

The block diagram for this controller, Fig. 8, shows again that the feedforward path takes the difference between two open-loop transfer functions. This time, however, both of these transfer functions represent positions remote from the actuator force. Note that the auxiliary output is x_1, which is not a measurable position.

The root locus plot, Fig. 9, shows a very interesting effect. The system is only conditionally stable. For low values of k_f, the system is stable; for high values of k_f, the system is unstable; and for some critical value of the force feedback gain, the system is only marginally stable. The ± 60-deg asymptotes result from the system's having *six* open-loop poles, but only *three* open-loop zeros. Inspection of the open-loop transfer functions confirms this: The numerator of the transfer function relating $X_2(s)$ to $F(s)$ is a third-order polynomial in s.

To provide some physical interpretation to this effect, note again that the input force F is applied to m_1, which moves with x_1. The sensor is attached to the robot at m_2, which moves with x_2. Here the controller attempts to regulate the contact force *through* the m_2-

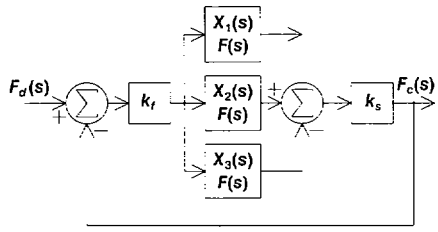

Fig. 8. Block diagram for the controller of Fig. 7.

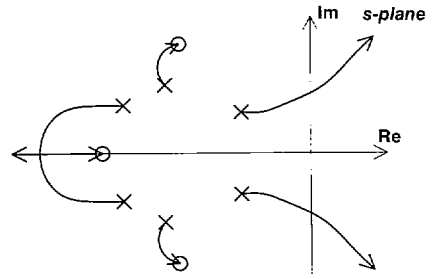

Fig. 9. Root locus plot shape for the controller of Fig. 7.

b_2-k_2 dynamic system. In the preceding two examples, stability was achieved while the controller regulated the contact force on the single-robot mass. In practice, gains are chosen to give stable response for nominal values of the workpiece parameters. Unstable behavior can then be observed with variations in those parameters. This instability can be predicted by drawing a new root locus plot for the varied system parameters.

Exclude Workpiece Dynamics

To determine the influence of the workpiece dynamic characteristics on this system, their effects are now removed from the model. Figure 10 shows the workpiece modeled rigidly as a "wall." The robot model still includes both the rigid-body and first vibration modes. The sensor consists of a spring and damper between the robot and the workpiece.

This simpler two-mass model has only two state variables, x_1 and x_2, which measure the displacements of the two robot masses. The two open-loop transfer functions are

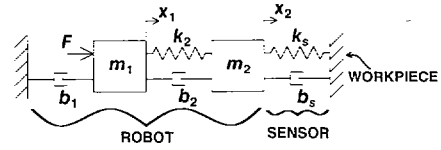

Fig. 10. Robot system model including robot first-mode and rigid workpiece.

$$X_1(s)/F(s)$$

$$= [m_2 s^2 + (b_s + b_2)s + (k_s + k_2)]/D_4^*$$

$$X_2(s)/F(s) = [b_2 s + k_2]/D_4^*$$

where

$$D_4^* = [m_1 s^2 + (b_1 + b_2)s + k_2]$$

$$\cdot [m_2 s^2 + (b_2 + b_s)s + (k_2 + k_s)]$$

$$- [b_2 s + k_2]^2$$

The contact force is given by

$$F_c = k_s x_2$$

and the control law again will be

$$F = k_f(F_d - F_c), \quad k_f \geq 0$$

The block diagram for this controller, Fig. 11, shows that *no* differences in open-loop transfer functions are being taken.

The root locus plot is shown in Fig. 12. Again, the system is conditionally stable, as this time there is *one* open-loop zero and *four* poles. The instability is therefore shown to be present regardless of the workpiece dynamics (which may have been suspect in the preceding case of the model in Fig. 7).

Comparison of the two-mass model of Fig. 4 with that of Fig. 10 shows that the models are basically the same (note the different subscripts), and the equations are therefore of the same form. One controlled system is stable (Fig. 6), however, while the other is not (Fig. 12). The difference is only in the placement of the sensor. In the former, the feedback comes from the spring *between* the masses. In the latter, the feedback signal comes from the spring at the second mass to ground. A typical industrial robot with first mode near 20 Hz and a stiff force sensor may have the following parameters: $m_1 = 40$ kg, $m_2 = 40$ kg, $k_2 = 400{,}000$ N/m, $k_s = 315{,}000$ N/m, $b_1 = 500$ N-sec/m, $b_2 = 500$ N-sec/m, $b_s = 400$ N-sec/m. For a very stiff workpiece, the upper limit on gain for stability is $k_f = 1.16$.

Conclusion

A series of lumped-parameter models has been developed in order to understand the effects of robot and workpiece dynamics on the stability of simple force-controlled systems. An instability has been shown to exist for robot models that include representation of a first resonant mode for the arm. The mode modeled can be attributed to either drive train or structural compliance (or both). The potential for instability is present because the sensor is then located at a point remote from the actuator. The controller attempts to regulate contact force through a dynamic system. Compare the systems of Figs. 7 and 10 with those of Figs. 1 and 4.

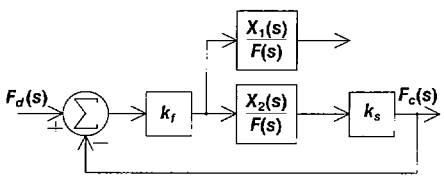

Fig. 11. Block diagram for the controller of Fig. 10.

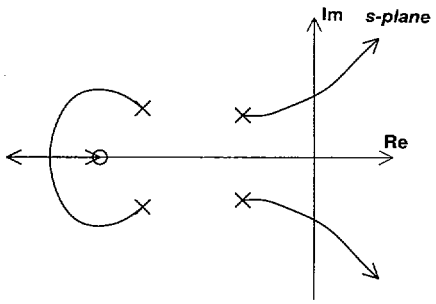

Fig. 12. Root locus plot shape for the controller of Fig. 10.

It must be noted, however, that there are many causes of force-controlled instabilities. The effect presented in this article, that of robot structural dynamics, is an important problem in some systems. If the desired closed-loop bandwidth is low compared to the first mode frequency of the arm, then the target performance may be achievable. However, if we require a machine capable of higher performance, we must also investigate other issues carefully. In particular, the workpiece dynamics, higher structural modes, actuator limitations, and controller implementation must be considered.

The effect of the workpiece dynamics is as yet unclear. Observation of force-controlled robotic systems suggests that the workpiece, when coupled through the force sensor, can significantly change the dynamics. Certainly, if the workpiece were very compliant and extremely light, there could be no force across the sensor, degenerating the closed-loop system to the open-loop case, which of course is stable. In this article, we have demonstrated the opposite extreme, that when the workpiece is modeled as a rigid wall, the system can be unstable. The sensor and workpiece (environment) dynamics are therefore important and should be modeled. Limited actuator bandwidth, filtering, and digital controller implementation can also cause instability. These performance limitations must also be included in the system model used for controller design.

In this article, we have not addressed the nonlinear effects of the discontinuity at the workpiece contact, the associated impact forces that occur, axis friction, joint backlash, or actuator saturation. Nonlinear simulations suggest, however, that these effects can, under some conditions, lead to limit cycles in the otherwise stable linear systems, and under other conditions, they can even stabilize unstable linear systems. The stability bounds derived using the linear models should be used to set upper limits on the controller gains, which should then be decreased if limit cycles are observed under operating conditions.

The modeling and analysis techniques presented are tools to aid in control system design. For their accurate use, however, the models must sufficiently describe the actual hardware. A topic of ongoing research is the comparison of these model predictions with experimental result.. In particular, it is not clear how all the model parameters should be chosen in order to assure agreement between the analytical model and the experimental hardware.

References

[1] S. D. Eppinger and W. P. Seering, "On Dynamic Models of Robot Force Control," *Proc. Int. Conf. Robot. Autom.*, Apr. 1986.

[2] D. E. Whitney, "Historical Perspective and State of the Art in Robot Force Control," *Proc. Int. Conf. Robot. Autom.*, Mar. 1985.

[3] M. T. Mason, "Compliance and Force Control for Computer Controlled Manipulators," *IEEE Trans. Syst., Man, Cyber.*, vol. SMC-11, pp. 418–432, June 1981.

[4] M. H. Raibert and J. J. Craig, "Hybrid Position/Force Control of Manipulators," *J. Dyn. Syst., Measurement and Control*, vol. 103, June 1981.

[5] J. K. Salisbury, "Active Stiffness Control of a Manipulator in Cartesian Coordinates," *Proc. 19th Conf. Decision and Control*, vol. 1, Dec. 1980.

[6] D. E. Whitney, "Force Feedback Control of Manipulator Fine Motions," *J. Dyn. Syst., Measurement and Control*, vol. 99, pp. 91–97, June 1977.

[7] N. Hogan, "Impedance Control of Industrial Robots," *Robotics and Computer-Integrated Manufacturing*, vol. 1, no. 1, pp. 97–113, 1984.

[8] J. L. Nevins and D. E. Whitney, "The Force Vector Assembler Concept," *Proc., First CSIM-IFTOMM Symp. Theory and Practice of Robots and Manipulators*, ASME, Udine, Italy, Sept. 1973.

[9] Y. H. S. Luh, W. D. Fisher, and R. P. C. Paul, "Joint Torque Control by a Direct Feedback for Industrial Robots," *IEEE Trans. Auto. Contr.*, vol. AC-28, Feb. 1983.

[10] R. K. Roberts, R. P. Paul, and B. M. Hillberry, "The Effect of Wrist Force Sensor Stiffness on the Control of Robot Manipulators," *Proc. Int. Conf. Robot. Autom.*, Mar. 1985.

[11] W. B. Gevarter, "Basic Relations for Control of Flexible Vehicles," *AIAA J.*, vol. 8, no. 4, pp. 666–672, Apr. 1970.

[12] R. H. Cannon and E. Schmitz, "Initial Experiments on the End-Point Control of a Flexible One-Link Robot," *Int. J. Robot. Res.*, vol. 3, no. 3, pp. 62–75, Fall 1984.

[13] L. M. Sweet and M. C. Good, "Redefinition of the Robot Motion Control Problem," *IEEE Cont. Syst. Mag.*, pp. 18–25, Aug. 1985.

Steven D. Eppinger received the S.B. degree in 1983 and the S.M. degree in 1984 from the Massachusetts Institute of Technology, Department of Mechanical Engineering. He is now a candidate for the Ph.D. degree and is conducting research at the MIT Artificial Intelligence Laboratory. Mr. Eppinger's research interests lie in the area of automated manufacturing, specifically improving machine performance with sensory information and computation.

Warren P. Seering received the B.S. degree in 1971 and the M.S. degree in 1972, both from the University of Missouri at Columbia. He continued his graduate work at Stanford University, receiving the Ph.D. degree in 1978. In Fall 1978, Professor Seering was appointed to the faculty of the Department of Mechanical Engineering at the Massachusetts Institute of Technology. His work has focused on machine design and the role of computation in machine performance. Professor Seering helped to establish the MIT Machine Dynamics Laboratory, of which he is currently Co-Director. Professor Seering is now conducting research at the MIT Artificial Intelligence Laboratory. His research interests are in the areas of dynamics, vibration, system design, and artificial intelligence. His work centers around the use of computation to extend the performance of machines, particularly robots.

1987 CDC

The IEEE Conference on Decision and Control (CDC) is the annual meeting of the IEEE Control Systems Society and is conducted in cooperation with the Society for Industrial and Applied Mathematics (SIAM) and the Operations Research Society of America (ORSA). The twenty-sixth CDC will be held on December 9–11, 1987, at the Westin Century Plaza Hotel in Los Angeles, California. The General Chairman of the conference is Professor William S. Levine of the University of Maryland. The Program Chairman is Professor John Baillieul of Boston University. The conference will include both contributed and invited sessions in all aspects of the theory and application of systems involving decision, control, optimization, and adaptation.

We urge you to attend this premier control conference held in the dynamic and historic setting of Los Angeles. The pictures here illustrate a few of the many attractions of the Los Angeles area. For further information, contact the General Chairman:

Prof. William Levine
Dept. of Electrical Engrg.
University of Maryland
College Park, MD 20742
Phone: (301) 454-6841

The beautiful Malibu Beach community, embraced by the Pacific Ocean.

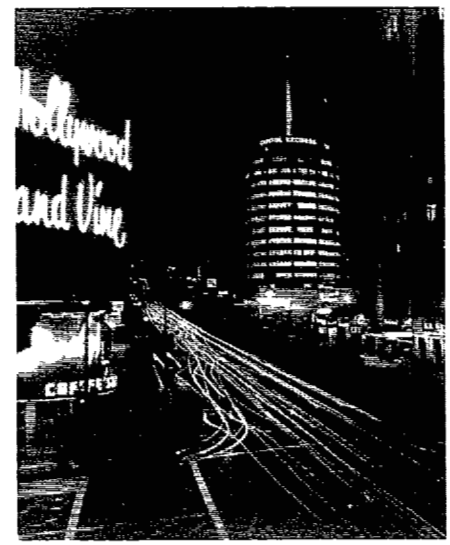

Hooray for Hollywood! This famous intersection of Hollywood and Vine is a focal point for the mystique of the Entertainment Capital. The Capitol Record Company in the background offers tours and shows how records are made.